Coefficient of Variation of Shear Strength of RC Beams and Size Effect

Wen Luo[1]; Jia-Liang Le, M.ASCE[2]; Mohammad Rasoolinejad[3]; and Zdeněk P. Bažant, Hon.M.ASCE[4]

Abstract: In shear failure, reinforced concrete (RC) beams always develop, in a stable manner, a finite length crack before the maximum load is reached. Thus, the crack tip location cannot sample a large volume of material with random strength because a small region in which the crack tip can lie is fixed by fracture mechanics. Consequently, the size effect on the mean strength cannot be statistical. It must be predominantly energetic or deterministic and, thus, must follow the Type-2 size effect law. What has not yet been clarified is the size effect on the coefficient of variation (CoV) of beam strength, which is important for anchoring the probability distribution of shear strength and choosing the safety factor. In this study, we run thousands of explicit finite element simulations using Abaqus-Explicit version 6.14 with microplane model M7, each with a random input of material strength and Young's modulus for each finite element in the structure. The CoV of beam strength is found to decrease with the structure size when geometrically similar beams are compared, although the CoV tends to a constant for large sizes. This size effect on the CoV is similar to that in ductile failure governed by a Gaussian distribution of strength and contrasts with that in brittle failures following the Weibull distribution, for which the CoV is size independent. To characterize the size dependence of the strength CoV, an analytical formula is developed based on the statistics of the sample quantiles of a series of random variables. **DOI: [10.1061/(ASCE)EM.1943-7889.0001879](https://doi.org/10.1061/(ASCE)EM.1943-7889.0001879).** *© 2020 American Society of Civil Engineers.*

Introduction

The reliability of reinforced concrete (RC) structures is a major concern in modern structural design. When assessing the strength and reliability of RC beams, one crucial aspect size is the size effect. How structural strength scales with structure is already known reasonably well (Bažant and Yu 2009). However, how does the strength scatter scale?

A large majority (in fact, 87%) (Yu et al. 2016) of all available laboratory test data are based on relatively small beams, with a depth smaller than 20 in. (508 mm), whereas in practice, much larger beams are critical and often designed. Due to this discrepancy between laboratory and practice, relying on a theoretical and realistic size effect law to extrapolate from smaller beams tested in the lab to much larger ones in practice is inevitable.

When studying the deterministic failure of quasi-brittle materials, two types of size effects exist on structural strength. The Type 1 size effect (Bažant and Yu 2009; Yu et al. 2016; Dönmez and Bažant 2019) occurs in structures that fail (under load control) catastrophically as soon as a macrocrack initiates somewhere in the structure.

Particularly relevant to the current paper is the Type 2 size effect law (Bažant and Kazemi 1990; Bažant 1984), which is typical for RC structures and has recently been incorporated into the ACI design code (ACI 2019) for beam shear, punching, and strut-and-tie design. The Type 2 size effect occurs when geometrically similar cracks develop stably prior to the peak load, which is common for RC structures due to the reinforcement action (Kim and Park 1994; Kwak et al. 2002; Kuo et al. 2014; Chao 2020; Daluga et al. 2017; Sherwood 2008; Mahmoud and El-Salakawy 2016; Ghannoum 1998). It also applies to specimens with pre-existing large notches. The Type 2 size effect is caused by the size dependence of the strain energy release rate due to crack advance at the critical state of maximum load.

Apart from the deterministic size effect laws, also important is the statistical size effect that arises from the random heterogeneity inherent to the material (Le et al. 2011; Bažant 2002). This leads to a scaling relation for the mean strength and its coefficient of variation (CoV). Knowing such scaling is necessary to evaluate the reliability of engineering structures, especially at the one-out-of-one-million (10^{-6}) failure risk level required for structural safety.

In concrete, its heterogeneity and the irregular geometry of grains lead to considerable variability in the overall structural response. As is typical of quasi-brittle materials, the strength of plain concrete follows the Gauss-Weibull statistical size effect. This size effect means that the strength decreases as the structure size grows, terminating with the asymptotic slope $-n/m$ in the plot of the log-mean of strength versus log D. Here, m is the Weibull modulus, and $n = 1, 2$, or 3 is the number of spatial dimensions in which the structure is scaled. For not too wide beams, the proper choice is $n = 2$ because the shear fracture must advance simultaneously through the entire beam thickness. The CoV of material strength is a constant for the large size limit, which is a consequence of the Weibull tail of the strength distribution.

The Weibull statistical size effect is not directly applicable to reinforced concrete structures. Because of the reinforcement effect, the fundamental hypothesis of Weibull statistics (Fisher and Tippett 1928; Weibull 1939; Bertin and Györgyi 2010) is invalid—the local

[1]Graduate Research Assistant, Dept. of Civil and Environmental Engineering, Northwestern Univ., Evanston, IL 60208

[2]Associate Professor, Dept. of Civil, Environmental, and GeoEngineering, Univ. of Minnesota, Minneapolis, MN 55455. ORCID: https://orcid.org/0000-0002-9494-666X

[3]Graduate Research Assistant, Dept. of Civil and Environmental Engineering, Northwestern Univ., Evanston, IL 60208. ORCID: https://orcid.org/0000-0003-3387-3580

[4]McCormick Institute Professor and W.P. Murphy Professor of Civil and Mechanical Engineering and Materials Science, Northwestern Univ., Evanston, IL 60208 (corresponding author). Email: z-bazant@northwestern.edu

failure of any representative volume element (RVE) can no longer trigger a catastrophic failure of the entire structure. Because the reinforcement stabilizes the shear crack propagation, the peak load is reached only after the growth of a long crack. Consequently, the strength variability and its statistical distribution do not follow Weibull statistics and need to be studied.

As the continuation of a previous work in ICOSSAR proceedings (Bažant et al. 2013), this paper studies the scaling of the failure probability of RC beams without stirrups and analyzes the CoV of structure strength. We first introduce the concept of sample p-quantiles (Walker 1943; Stigler 1973; Mood 1950; Samuel-Cahn 1994; Leadbetter et al. 2012) of strength statistics to model the failure probability of RC beams, and then combine it with Monte Carlo numerical simulations. Finally, we analyze the large size limit of the CoV of strength that helps evaluate the reliability of reinforced concrete structures.

For the numerical simulations of stochastic damage and crack evolution in quasi-brittle materials, the discrete models (Bolander and Saito 1998; Cusatis et al. 2011) have been favored because they can directly represent a lattice system with the randomly irregular intergranular connectivity on the mesoscale. Some valuable qualitative findings on random behavior can be obtained from such simulations. For instance, a large amount of microcracks are found at the peak load in plain concrete simulations (Man and Van Mier 2011). The randomness in notched beams affects only the variability of their strength but not the mean behavior (Eliáš et al. 2015). Replication of the mesoscale structure of concrete in these models helps obtain realistic results. However, this comes at the price of the high computational cost of the simulations of large structures.

To reduce the computational cost and enable running fast enough numerous Monte Carlo experiments, we opt for an explicit model, the microplane model M7 (Caner and Bažant 2013a, b) embedded in the framework of finite element analysis. Instead of modeling the random intergranular connectivity on the mesoscale, we use regular finite elements with random material properties to account for the material heterogeneity of concrete. The random properties are sampled from a Gauss-Weibull distribution with the m-value (Weibull modulus) being less than the macroscale value of 24 according to the hierarchical probabilistic model (Bažant and Pang 2006, 2007; Le et al. 2011).

For mechanicians, the term "beam shear" calls for an explanation. The shear crack actually grows as a Mode I (opening) crack. It is called a shear crack because it is created by shear force in the RC beam.

Model Configuration

Because the size effect is a quintessential property of concrete fracture, we consider beams of three total depths: $H_1 = 200$ mm, $H_2 = 400$ mm, and $H_3 = 800$ mm (Fig. 1). The corresponding effective beam depths (from top face to steel centroid, excluding the concrete cover) are $D_1 = 160$ mm, $D_2 = 360$ mm, and $D_3 = 740$ mm. The beams of all sizes are geometrically similar in two
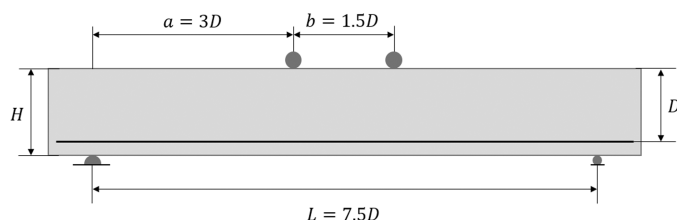

Fig. 1. Geometry of RC beam.

dimensions; that is, only the lengths and depths are scaled, whereas the thickness b is kept constant at 20 mm. This avoids the minor but nonnegligible wall effect, which would complicate the evaluation. The choice of dimensions is based on important previous test data for shear failure of reinforced concrete (RC) beams (Syroka-Korol et al. 2014). Because the concrete cover, $H - D$, does not appreciably contribute to the beam strength, D rather than H is considered as the characteristic dimension. The relative shear span $a/D = 3$ is kept constant to ensure geometric scaling.

The RC beams are subjected to four-point loading under displacement control. For simplicity, the rebar is modeled by truss elements using Young's modulus of 200 GPa. The truss elements' nodes rigidly attached to the concrete elements' nodes. To reduce the computational cost, the reinforcing bar is attached to only one surface of the specimen on which the boundary condition of symmetry is applied; thus, the equivalent specimen thickness is 40 mm. The reinforcement ratio ρ is set to 1.2% for all three beam sizes and is chosen the same as in the experiments in (Syroka-Korol et al. 2014). This ratio prevents the steel from yielding. As a consequence, almost all specimens fail right after the peak load if load control is used. The simulation results subsequently indicated here confirm this behavior.

In simulations with the crack band model (Bažant and Oh 1983; Bažant and Planas 1998), which we adopt to avoid spurious mesh sensitivity, the element size is dictated by the fracture energy, G_f. Based on the aggregate size and experience with typical concrete, we use finite cubical elements of dimensions $20 \times 20 \times 20$ mm. The element type is C3D8R, that is, a cubic element with reduced integration. The damage constitutive law of concrete is the microplane model M7, which is implemented in ABAQUS as a VUMAT subroutine for damage and failure of concrete (Caner and Bažant 2013a, b).

Young's modulus, E, and radial scaling parameter, k_1, of the microplane model, which jointly controls material compression strength, are here randomized on the basis of the grafted Gauss-Weibull distribution (Le et al. 2011; Bažant and Pang 2007). Even though both Young's modulus and strength are random, they are strongly correlated. For simplicity, we consider them to be perfectly correlated, related by the approximate ACI formula $E = 4735\sqrt{f_c'}$ (f_c, E in psi). This means that, for instance, an element of high strength will also have a high Young's modulus. Furthermore, based on experience, we assume the autocorrelation length of the random field to be equal to the width of the fracture process zone, which is approximatley equal to the element size. Therefore, the autocorrelation need not be considered in the finite element simulations as long as the element size does not change, which applies here.

At the beginning of each run, random numbers are first generated for each element (and for each Gauss point due to reduced integration). They are based on a grafted distribution with Gaussian core of mean $\mu = 9$ and standard deviation $s = 1.843$, and with a remote lower Weibull tail.

Because the magnitude of the M7 model parameter k_1 in deterministic simulations is on the order of 10^{-4}, the random value of k_1 for each element is evaluated by dividing the generated random numbers by 10^5. Young's moduli are generated in a similar fashion. To guarantee that each element has a unique pair of randomized strength and modulus, the random properties are assigned according to the element index that has passed into the VUMAT subroutine.

Fig. 2 indicates one random realization of the material properties of the beam. To visualize the result, the dimensionless random number is stored in the state variable SDV190 in Abaqus. The darker the shade, the stronger (and also stiffer) the element. Apart from the
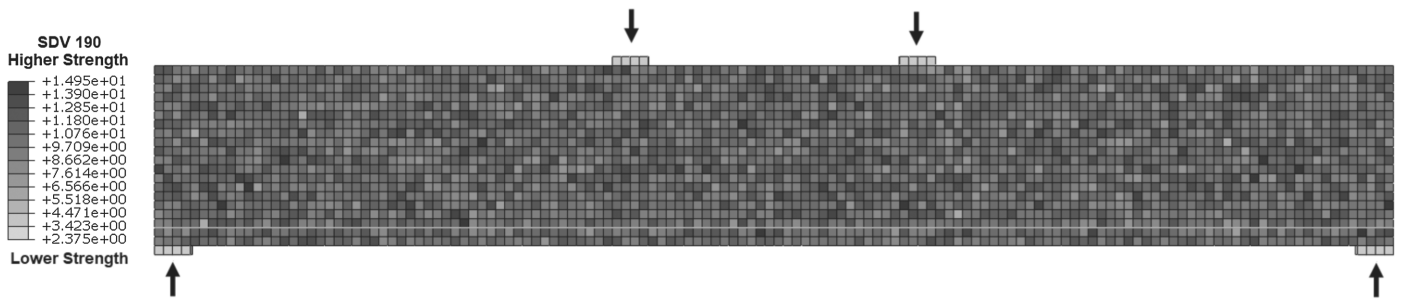
Fig. 2. One realization of random strength and modulus of median-size RC beam ($H = 400$ mm). The darker the shade, the stronger the element (in terms of strength and stiffness).

Table 1. Microplane M7 model parameters for concrete

| Parameter	Value
E (MPa)	$\sim 2.5 \times 10^4$
ν	0.18
k_1	$\sim 1 \times 10^{-4}$
k_2	110
k_3	30
k_4	100

randomized model parameter k_1, other major M7 parameters are given in Table 1.

For each beam size, one thousand Monte Carlo finite element simulations of shear failure with random parameters were run. The maximum shear forces V are obtained from the recorded load-displacement curves, after which they are normalized to the nominal strength of the beam according to $\sigma_N = V/bD$, where $b =$ beam thickness.

Size Effect on Mean and CoV of Nominal Shear Strength

Is Crack Growth a Random Process?

The diagonal shear crack initiates at the longitudinal reinforcement at the bottom of the beam and then propagates upwards in a stable manner under increasing load. At peak load, the crack front lies approximately at a $0.2D$ distance from the top face of the beam. The location of the crack initiation at the bottom is random over a much broader range, as observed in Fig. 3, in which the crack paths from tests at various beams sizes, scaled to one size, are collected. In perfunctory discussions, it was sometimes thought that the crack
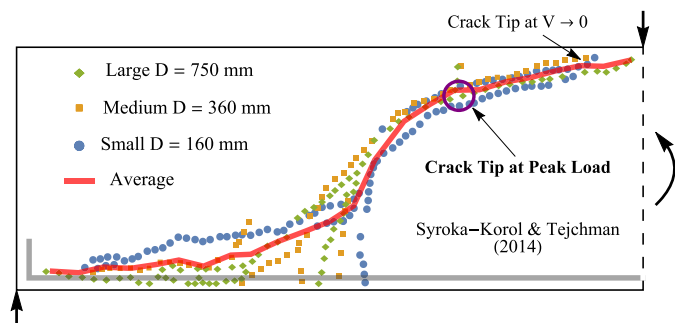
should be treated like a Markov process, or some other random process, leading to an even greater spread of the random tip locations at peak load.

However, the opposite is true, as experimentally best demonstrated by Syroka-Korol and Tejchman; see Fig. 3. If no random scatter is considered, fracture mechanics forces the crack tip to lie at peak load at a certain precise location. If the random scatter is considered, fracture mechanics forces the tip to lie in a relatively small region—much smaller than the region of crack initiation points at the bottom. Thus, the cracks widely scattered at the bottom tend to converge to this region. Therefore, the random spread of the crack tip location at peak load is much smaller than the random spread of the crack initiation point. Therefore, random process modeling of shear crack growth would not be realistic unless subordinated to fracture mechanics, which would be difficult and is unnecessary.

Mean Size Effect on Strength

Despite the randomness considered in the model, we must consider the mean behavior of the RC beam to be dominated by the quasi-brittle fracture mechanics (Bažant and Kazemi 1990; Bažant and Planas 1998) and analyze it deterministically. Fig. 4 indicates the idealized diagonal shear crack at peak load. As argued in Bažant (1997) and demonstrated in Yu et al. (2016) and Dönmez and Bažant (2019), the tensile stress across the crack (called aggregate interlock stress), as well as the Mode I fracture energy, is at peak load reduced virtually to zero, and the failure at peak load is caused by crack-parallel compression. This is documented by the field of vectors of principal compressive stress at peak load, computed in (Dönmez and Bažant 2019) and displayed in Fig. 5. The shear-compression crushing of element Δa in Fig. 4 causes a slip of the cross-hatched wedge-shaped zone and diminishes the compression stress and strain energy in that wedge.

Fig. 3. Crack patterns documented in scaled beams of different sizes.
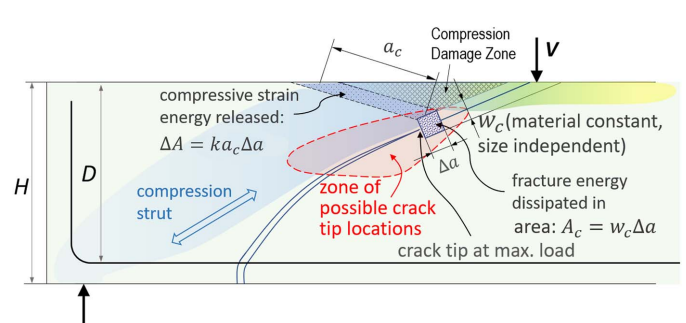
Fig. 4. Idealized intuitive fracture increment at peak load.
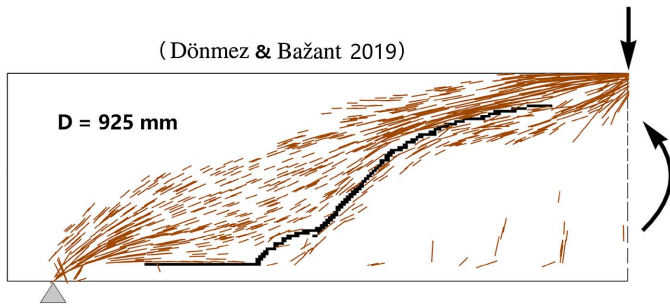
Fig. 5. Minimum principal compressive stresses in RC beam.

Imagine the shear crack to extend by the distance Δa. Similar to all quasi-brittle materials, the width, w_c, of the fracture process zone (FPZ) of the crack, simulated as a propagating crack band, is approximately a material constant and is size independent. To satisfy the energy balance of the fracture process, the elastic energy released in the entire structure during incremental crack advance Δa must equal (per unit beam thickness) the work of the fracture dissipated by Δa

$$-\bar{U}(\Delta A_c + \Delta A) = G_f w_c \Delta a \qquad (1)$$

where $\bar{U}$ = strain energy increment at peak load; A = area of major strain energy release; ΔA_c = area of increment crack band; and G_f = average fracture energy of concrete (mixture of mode-I). The region of significant energy release is a band above the crack increment (see shaded area in Fig. 4). We then express the average energy density change as $C\sigma_N^2/2E$, where C = constant due to geometric similarity, to take account of the spatial variation of the strain energy. Let the length of the energy relief band be a_c; then, Eq. (1) reduces to

$$C\frac{\sigma_N^2}{2E}(ka_c\Delta a + w_c\Delta a) = G_f w_c \Delta a \qquad (2)$$

where k = direction cosine that projects Δa to the width direction of the compressive strain energy release band. Rearranging Eq. (2) and leaving σ_N on the left gives

$$\sigma_N = \frac{\sigma_0}{\sqrt{1 + D/D_0}} \qquad (3)$$

where $\sigma_0 = \sqrt{2EG_f/C}$, $D_0 = w_c/(k\alpha_c)$, and $\alpha_c = a_c/D$. This is the classical Type 2 deterministic size effect (Bažant 1984; Bažant and Kazemi 1990; Bažant 2002). Note that Young's modulus E and fracture energy G_f are actually random variables for each element; therefore, the quantities in this mean size effect relation [Eq. (3)] are their expected values.

Size Effect of CoV of Strength

Sample p-Quantiles
Although the size effect on the mean shear strength of RC beams is dictated by fracture mechanics, the scatter of nominal strength, in terms of the variance and coefficient of variation, is rooted in the randomness of the material. We start from the mean size effect relation, Eq. (3), and allow its parameters to take random values. For instance, we let $\sigma_0 = \sqrt{2EG_f/C}$ be random, where E and G_f no longer take the mean values. Because the parameters in the size effect relation do not refer to an arbitrary element in the structure

but to the critical shear crack increment when the peak load is reached, we cannot directly use in our model the distribution of E and G_f previously defined for every single finite element.

The critical element that triggers the peak load only shows up in a relatively small region along the major diagonal shear crack close to the load point on top. To get the size effect on the strength CoV, we first need a rough estimate of the probability distributions of the local material parameters critical for σ_0 and D_0 in the size effect relation. As the shear crack propagates, its local crack tip trajectory tends to grow in the direction of relatively weak elements in the randomly heterogeneous material, making the crack trajectory possibly deviate from the direction of the maximum tensile stress. In contrast, the overall crack trajectory must still roughly follow the deterministic solution, which is governed by fracture mechanics.

As a consequence, the properties of the extremely strong elements do not directly affect the peak load. The reason is that the critical element is very unlikely to be among those extremely strong ones unless the elements surrounding the crack tip are all strong, in which case it simply means that the mean strength is on the high side. In contrast, some extremely weak element is also unlikely to be the critical one because the elements neighboring the weak one are likely to be much stronger. Therefore, the overall load, as well as the nominal stress, will continue to increase as the crack keeps growing after the failure of an extremely weak element. Intuitively, neither the extremely strong nor the extremely weak elements determine the peak load.

Based on this reasoning, we adopt the p-th sample quantile, $\sigma_0(p)$ (where $0 < p < 1$), of n i.i.d. (independent identically distributed) random variables, to approximate the ductile limit of the Type 2 size effect, σ_0, in Eq. (3). The value of p should lie somewhere between the quantile limits, 0 and 1, standing for the weakest and strongest element in the structure. The sample size n represents the number of elements potentially critical for the peak load.

The distributions of sample quantiles are closely related to those of the order statistics. Both are random variables arising from an ordered list of random variables. The sample quantile is characterized by the relative order percentage (p) in the list of all variables, rather than the absolute order considered in the order statistics.

To further compare the two random variables, consider a list of i.i.d. random variables arranged in ascending order, $X_1, X_2, \ldots, X_n$, where $X_k = k$th order statistic. The sample p-quantile corresponds to the (np)th order statistic, X_{np}. Fig. 6 illustrates the relation of the limiting distributions of sample quantiles and order statistics. If we fix the order k and let $n \to \infty$, we obtain the limiting distribution of order statistics; whereas, if we fix the ratio $k/n = p$ and let the order k increase with n, we obtain the limiting distribution of the sample p-quantile, which is known to be the normal (or Gaussian) distribution regardless of the distribution of X_i [see Kendall et al. (1948)]. In the special case of $p = 0.5$, the corresponding sample quantile is simply the median of n i.i.d. random variables.

The strength of the critical element, σ_0, is approximated by the (np)th weakest element in the entire critical region. As the RC beam becomes larger, the size of the possible region for the critical crack tip, n, also grows. For increasing sample size n, the distribution of the p-th sample quantile converges to the normal distribution with mean $x_p = F^{-1}(p)$ and variance $p(1-p)/(nf(x_p)^2)$, where $f(x_p) = F'(x_p)$ is the value of the probability density function (p.d.f.) of material strength evaluated at the p-th theoretical quantile.

In cases the variation of D_0 is negligible compared with that of σ_0, we simply treat D_0 as a deterministic constant. Then, the nominal strength of the RC beam follows the asymptotically normal distribution
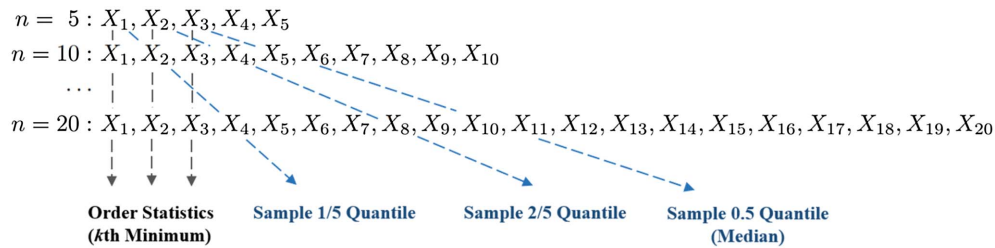
Fig. 6. Relation between sample quantiles and order statistics.

$$\sigma_N \sim N\left(\frac{F^{-1}(p)}{\sqrt{1 + D/D_0}}, \frac{p(1-p)}{nf(x_p)^2(1 + D/D_0)}\right) \qquad (4)$$

where $F(x)$ = cumulative distribution function of the element strength; and N = unit normal distribution function.

For cases in which the randomness of D_0 is not negligible, its effect on the scatter of σ_N is subsequently discussed. For the derivation of the distribution of sample quantiles of i.i.d. random variables, see Kendall et al. (1948).

Critical Region of Possible Crack Tip Locations

Since we are interested in the relation between the CoV of the nominal shear strength and the structure size D, the natural question is: How does the size of the critical region n of all possible crack tip locations scale with structure size D? There are three possibilities.

1. The critical region size, n, does not depend on structure size D and remains constant, in which case the critical region becomes negligibly small compared with the entire structure as D tends to infinity.
2. n is proportional to D^2, that is, the area of the critical region grows proportionally with the specimen area.
3. n increases with the growth of D but the rate is slower than D^2.

To figure out the correct case, we conduct FE Monte Carlo simulations of the RC beams and attempt to obtain the histogram of the vertical coordinates of the critical crack tips. Because the maximum principal log-strain (LE-MaxPrincipal in Abaqus) is normally used to indicate the location of a crack, we superimpose for each beam size the logarithmic strain field at peak load for all 1,000 random simulations and then take their average. This averaged superposition of strain fields reflects the relative likelihood (or probability density) that cracks/damages will appear at each location in the

beam given that elastic deformations are negligible relative to those due to crack opening. To focus on the vertical location distribution of the critical crack tip, we add up the strain values for each finite element in the same row after removing elements that remain purely elastic, as indicated by setting a threshold strain. Then, we obtain an average strain field that only depends on the vertical coordinate along the beam depth direction.

Note that many parallel cracks appear close to the dominant shear crack (Fig. 7) and that the crack density gradually decreases as widely spread parallel cracks at the bottom of the beam gradually localize into a single major diagonal shear crack when progressing toward the top. As a result, the summed strain continues to increase from the top to the bottom of the beam. It even grows below the reinforcement bar without plateauing.

Interpreting such a strain field as the cumulative probability for the location of the critical crack tip would lead to the wrong conclusion that the structural failure could be triggered by elements in the concrete cover at the bottom. To obtain the vertical location distribution purely for the critical diagonal crack tip, we must remove the strain contribution from the densely populated parallel cracks at the concrete cover.

To do so, we subtract from the summed strains a linearly increasing function of the distance measured from the top of the beam. The parameters of this linear function are chosen such that the strain values at the bottom of the beam plateau, whereas the entire function is still monotonically increasing. Finally, we normalize the summed strains for each row to the range of 0–1, such that it becomes a cumulative probability measure. By fitting the normalized strain field, we obtain a cumulative probability distribution function (c.d.f.) for the vertical location of the critical crack tip. The probability density can then be easily calculated by taking the derivative of the c.d.f.
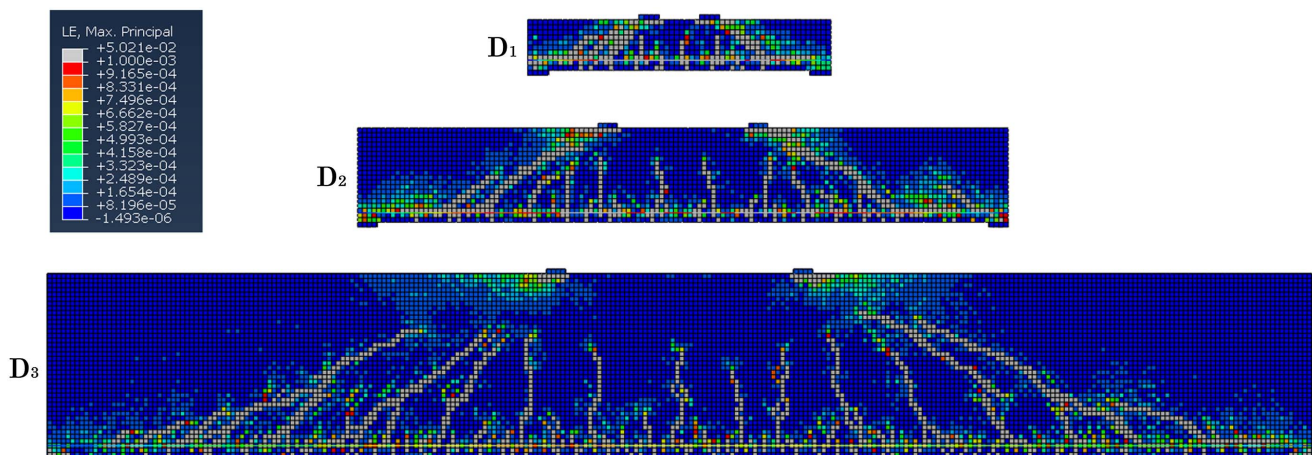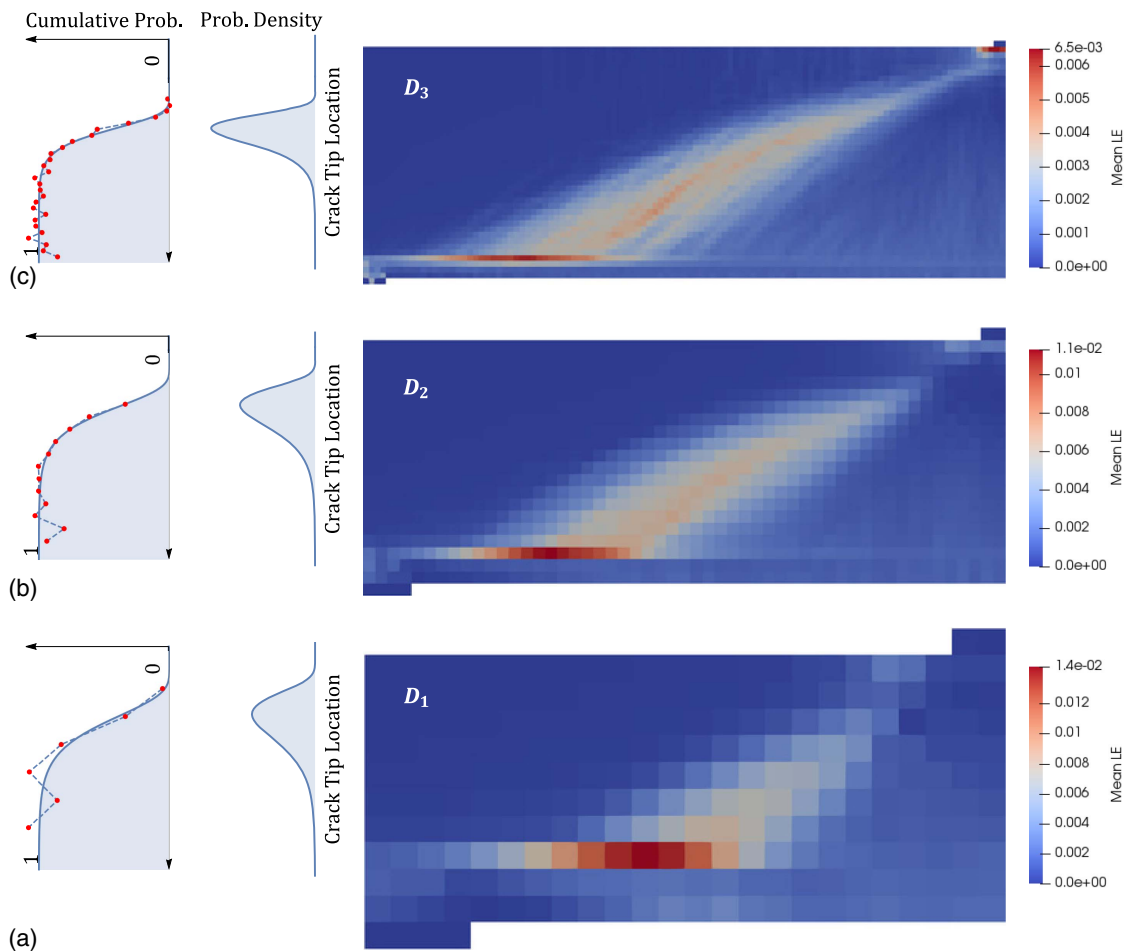

Fig. 7. Crack pattern of one random realization for each beam size.

Fig. 8. Average log strain field (LE) at peak load of 1,000 samples for each of the three beam sizes obtained by superposition: (a) smallest size D_1; (b) medium size D_2; and (c) largest size D_3. Indicated on the side are the probability density and cumulative distribution of the vertical location of the critical crack tip. The beams of three sizes are rescaled to the same size, for comparison. The mesh sizes are kept the same for all specimens, although they look different in this figure because of rescaling.

The visualization of the averaged strain field is conducted using Paraview version 5.5.2. Fig. 8 indicates the mean strain fields for specimens of three sizes and the fitted probability distribution of the vertical location of the critical crack tip. Now that we are interested only in the scatter (or standard deviation) of the crack tip location, it is not necessary to figure out exactly the type of distribution that it follows. Due to a slight positive skewness of the data (measured from top to bottom), we choose the lognormal distribution to fit it.

From this figure, one can observe that, as the structure size increases, the critical crack tip tends to concentrate on smaller regions after the structure is rescaled to the chosen reference size. In contrast, if we directly compare the distributions before rescaling, the standard deviation increases as the structure size grows. More specifically, the standard deviations for the scatter of the crack tip locations are 19.5, 32.0, and 44.4 mm for D_1, D_2, and D_3, respectively.

These observations indicate that the size of the critical crack tip region n grows as D increases, but the rate of growth is slower than D^2. Therefore, we replace n by $(kD)^c$, where $0 \leq c \leq 2$ is the exponent introduced to capture the growth rate of n as D increases; and k = ratio of the critical region height to D for the smallest beam. The typical value for k is approximately $1/4$. Then, substituting this into the variance of the nominal strength, we obtain its CoV by dividing the standard deviation by the mean:

$$\text{CoV}(\sigma_N) = \frac{\sqrt{p(1-p)}}{x_p f(x_p)}(kD)^{-c/2}, \quad \text{where } x_p = F^{-1}(p) \quad (5)$$

For simplicity, this formulation is based on one single sample p-quantile of the material strengths in the critical region. In reality, it could be a linear combination of several sample quantiles near the theoretical p-quantile. Then, the calculation of CoV must rely on the limiting joint distribution of different sample quantiles, which are multivariate normal distributions, but does not alter the critical scaling exponent $-c/2$ in the expression for the strength CoV. To see this, consider the limiting joint distribution of two different sample quantiles $X_{[np]}$ and $X_{[nq]}$:

$$\begin{bmatrix} X_{[np]} \\ X_{[nq]} \end{bmatrix} \xrightarrow{d} N \left(\begin{bmatrix} x_p \\ x_q \end{bmatrix}, \frac{1}{n} \begin{bmatrix} \dfrac{p(1-p)}{f(x_p)^2} & \dfrac{p(1-q)}{f(x_p)f(x_q)} \\ \dfrac{p(1-q)}{f(x_p)f(x_q)} & \dfrac{q(1-q)}{f(x_q)^2} \end{bmatrix} \right) \quad (6)$$

where the first vector is the mean, and the second matrix is the covariance matrix. The distribution of the linear combination of $X_{[np]}$ and $X_{[nq]}$ is essentially a double integral of the multivariate normal density function, in which the factor $1/n$ is a constant that carries over to the variance. Because $n \sim D^{-c/2}$, the scaling

exponent $-c/2$ is preserved even if σ_0 is the linear combination of several sample quantiles.

The current formulation bears some resemblance to that of the strength distribution of quasi-brittle fishnets (Luo and Bažant 2018; 2019). Indeed, by counting the damages at the peak load for either fishnets or fiber bundles under transverse scaling, it is clear that the average critical order k that determines the peak load increases linearly with the number of links n. In other words, their ratio $p = k/n$, which is the sample p-quantile of link strengths, tends to a constant.

As a result, the large size limiting strength distributions of both fishnets and fiber bundles are normal distributions. For the same reason, the strength distribution of RC beams in the present study also follows the normal distribution.

In contrast, the two cases are not exactly the same. For RC beams, the peak load will be triggered by material failure only in a small zone in the RC beam. However, for fishnets under uniaxial tension, the failure at any place in the structure could potentially lead to the peak load.

Strength Histogram

One thousand simulations have been run for each of the three beam sizes. The normalized load-displacement curves σ_N versus u/u_0 are shown in Fig. 9 [$\sigma_N = V/(bD)$, V = shear force]. The normalizing constant u_0 is chosen for each size such that all curves have the same initial stiffness. It is clear from the figure that both the critical load-point displacement and the peak load are random and that there is a size effect, that is, the nominal strength decreases as the structure size increases. All of the curves can be divided into four major sections according to the decrease in the slope, depicting four distinct stages of the failure process: (1) initial linear elastic response; (2) development of tensile cracks at the bottom of the beam; (3) development of the major diagonal shear crack (peak load); and (4) catastrophic failure of the entire RC beam if the load is controlled (postpeak). Additionally, the figure indicates that the scatter of the nominal strength decreases as the structure size increases.

Before analyzing the scatter of the nominal strength, we first verify the Type 2 size effect law (Bažant 1984; Bažant and Kazemi 1990) [Eq. (3)] for the mean strength of the RC beams. Eq. (3) can be rearranged to the linear regression plot (Bažant and Planas 1998)

$$y = Ax + C \tag{7}$$

where $x = D$ and $y = 1/\sigma_N^2$. The parameters σ_0 and D_0 in the size effect relation can be expressed in terms of A and C: $\sigma_0 = 1/\sqrt{C}$
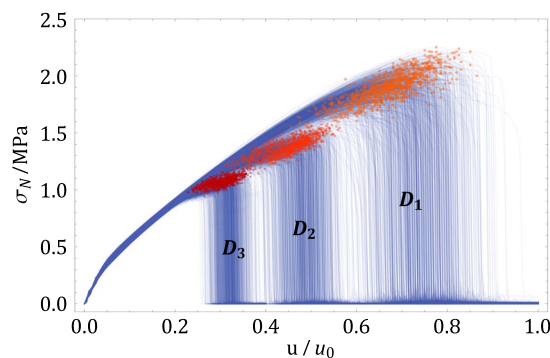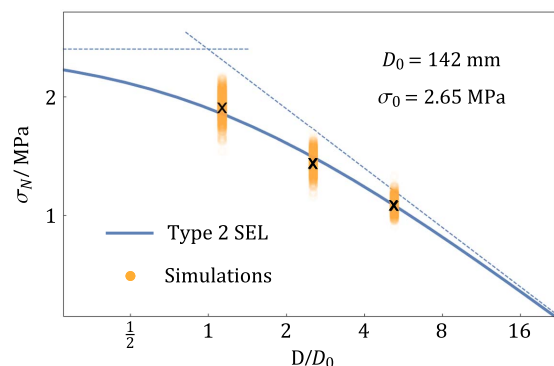
and $D_0 = C/A$. The optimal values for A and C obtained by fitting the simulated data of $1/\sigma_N^2$ are $A = 0.001006$ and $C = 0.143$, from which we obtain the values of the size effect parameters: $D_0 = 142$ mm and $\sigma_0 = 2.65$ MPa. Fig. 10 indicates the mean size effect curve of the scaling of RC beams together with all of the simulated beam strengths. Despite the randomness of the nominal strength, the mean value follows the Type 2 size effect as expected, confirming that such behavior is dominated by the deterministic energy release during diagonal crack propagation.

Fig. 11 indicates the histograms normalized to a probability density of the nominal shear strength for the three beam sizes. Indicated in the subplots on the right are the same histogram data in normal probability papers. The data form nearly straight lines for all three sizes, indicating that the histograms follow a normal distribution (although nothing can be inferred for the tails). The fitted normal distributions are plotted as solid curves on top of the histograms. The histograms clearly indicate that the variance of the nominal shear strength decreases as the structure size increases.

Because the mean strength also decreases as the structure size increases, we are interested in the change in the CoV, which is the standard deviation normalized by the mean. Therefore, we plot the CoV against D in a log-log scale (Fig. 12). Now, it is clear that the CoV also decreases as the structure size increases, which confirms the analysis based on the scatter of the critical crack tip location. The average slope in the log-log plot is -0.285.

To compare this with the classical statistical strength models, the infinite weakest-link chain model with Gauss-Weibull link strength distribution has a constant CoV under size scaling, and the fiber bundle model has a CoV that scales as $1/\sqrt{D}$. The slope of -0.285 found here for the RC beams lies between the slopes for these two models.

Worth noting is that the slope of the strength CoV for the RC beam is smaller in magnitude than the slope for the ductile fiber bundle. This is mainly because the size of the critical crack-tip region, n, does not grow linearly with the structure size, D, but rather $n \propto D^{0.57}$. Aside from the fact that the histograms follow normal distributions (Fig. 11), there clearly does not exist any "weakest-link" type behavior in the RC beams under shear loading. Otherwise, the tiny Weibull tail of the distribution of the inputs (k_1 and Young's modulus E) would dominate under the action of the weakest-link, leading to Weibull distributions for the nominal strength, which clearly is not the case. Despite the quasi-brittleness of concrete, the reinforcement prevents a sudden chain-like failure of the entire structure and ensures a stable propagation of the diagonal shear crack through approximately 80% of the cross-section depth up to the peak load. This is the major reason for the

Fig. 9. Normalized stress-displacement curves of 1,000 samples of structure of size D_2. Dark points indicate peak load locations.

Fig. 10. Size effect plot for two-dimensional scaling of RC beam. Solid curve indicates Type 2 size effect law (SEL) and overlapping circles are simulated nominal strengths (1,000 points for each size).
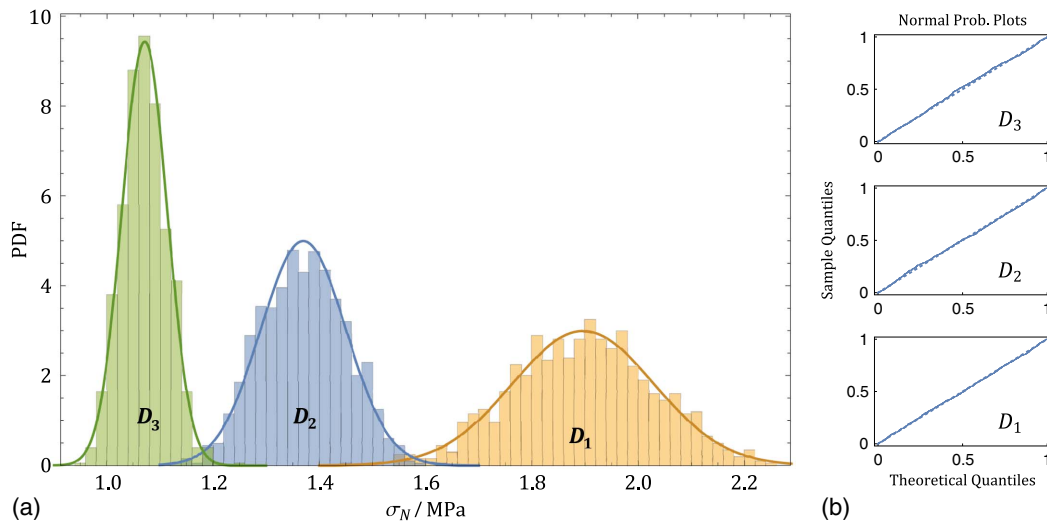
Fig. 11. (a) Histograms of nominal strengths for beams of three sizes (1,000 samples for each size); and (b) their normal probability plots.
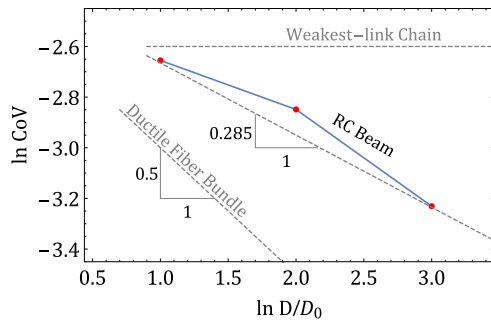
Fig. 12. Coefficient of variation (CoV) of shear strength of RC beams for three different beam sizes, and comparison with weakest-link model and fiber bundle model.

structure strength to have a Gaussian rather than a Weibull strength distribution.

Now that we know the scaling relation of CoV, we could use this information to roughly infer the quantile p that governs the strength of the beam using Eq. (5). The slope in the log-log plot, -0.285, corresponds to the exponent $-c/2$. Thus, $c = 0.57$. In other words, the number n of the potential critical crack tip locations scales as $D^{0.57}$.

Large Size Limit of Strength CoV

Up to now, we have studied the CoV of shear strength under the assumption that only σ_0 in Eq. (3) is random. This assumption is valid when D/D_0 is not too large compared with 1. Because of the square root and constant 1 in the denominator of the mean size effect relation, the effect of the randomness of D_0 is not as large as that of σ_0. In other words, the scatter of nominal shear strength σ_N is mainly affected by the randomness of σ_0 for small and medium-size RC beams. However, when the size increases, the effect of random D_0 could become nonnegligible.

Therefore, we need to study the large-size limit behavior of the RC beam by considering also the randomness of D_0. Because thousands of Monte Carlo simulations for extremely large RC beams would take an impractically long time to finish, we need a mathematical estimation of the scaling of strength CoV for extremely

large sizes. With the notation $D_0 = w_c/(k\alpha_c)$, Eq. (3) for $D \to \infty$ reduces to

$$\sigma_N \simeq \frac{\sigma_0 \sqrt{D_0}}{\sqrt{D}} \qquad (8)$$

In the expression of D_0, both the normalized length of the energy release band, α_c, and the characteristic length, w_c, could be considered as random variables. However, because the individual distributions of w_c and α_c are not known any better than that of D_0, it is appropriate to assign a distribution directly to D_0. Then, we analyze how the variance and CoV will change if D_0 in Eq. (8) is random. Because D_0, as the transitional size, refers to the entire structure, and D/D_0 is an indicator of the brittleness of the entire structure, the distribution of D_0 should not scale with the effective structure size D.

Denote the mean and variance of $\sqrt{D_0}$ by $\mu_{\sqrt{D_0}}$ and $s^2_{\sqrt{D_0}}$, and the mean and variance of σ_0 by μ_{σ_0} and $s^2_{\sigma_0}$. To estimate them, we first consider D_0 and σ_0 to be independent, and then the variance of the product $\sigma_0 \sqrt{D_0}$ can be calculated

$$\text{Var}(\sigma_0 \sqrt{D_0}) = \mathbb{E}[(\sigma_0 \sqrt{D_0})^2] - \mathbb{E}[\sigma_0 \sqrt{D_0}]^2 \qquad (9)$$

$$= \mathbb{E}[\sigma_0^2]\mathbb{E}[D_0] - \mathbb{E}[\sigma_0]^2 \mathbb{E}[\sqrt{D_0}]^2 \qquad (10)$$

$$= (s^2_{\sigma_0} + \mu^2_{\sigma_0})(s^2_{\sqrt{D_0}} + \mu^2_{\sqrt{D_0}}) - \mu^2_{\sigma_0}\mu^2_{\sqrt{D_0}} \qquad (11)$$

Because we assumed that the distribution of D_0 does not scale with size D, we let $\alpha = \mu^2_{\sqrt{D_0}}$ and $\beta = s^2_{\sqrt{D_0}}$. The variance of the product reduces to

$$\text{Var}(\sigma_0 \sqrt{D_0}) = (\alpha + \beta)(s^2_{\sigma_0} + \mu^2_{\sigma_0}) - \alpha\mu^2_{\sigma_0} = (\alpha + \beta)s^2_{\sigma_0} + \beta\mu^2_{\sigma_0} \qquad (12)$$

Following from $\mu_{\sigma_0} = x_p = F^{-1}(p)$ and $s^2_{\sigma_0} = p(1-p)/(nf(x_p)^2)$, this expression can be rewritten as

$$\text{Var}(\sigma_0 \sqrt{D_0}) = (\alpha + \beta)p(1-p)/(nf(x_p)^2) + \beta x_p^2 \qquad (13)$$

Using Eq. (13), the standard deviation of σ_N can be obtained by multiplying the square root of variance Var $(\sigma_0 \sqrt{D_0})$ with the factor $1/\sqrt{D}$

$$s_{\sigma_N} = \frac{\sqrt{(\alpha+\beta)p(1-p)/(nf(x_p)^2) + \beta x_p^2}}{\sqrt{D}} \qquad (14)$$

Meanwhile, the mean value of σ_N follows the large size limit of the Type 2 size effect, which is essentially the size effect of linear elastic fracture mechanics (LEFM)

$$\mu_{\sigma_N} = \mathbb{E}[\sigma_0 \sqrt{D_0}/\sqrt{D}] = \frac{\sqrt{\alpha} x_p}{\sqrt{D}} \propto D^{-1/2} \qquad (15)$$

Normalizing the standard deviation of σ_N by its mean provides the large-size scaling relation for the strength CoV

$$\mathrm{CoV}(\sigma_N) = \frac{s_{\sigma_N}}{\mu_{\sigma_N}} = \sqrt{\frac{(1+\beta/\alpha)p(1-p)}{nx_p^2 f(x_p)^2} + \beta/\alpha} \qquad (16)$$

where $\sqrt{\beta/\alpha} = \mathrm{CoV}(\sqrt{D_0})$, which is a constant. As $D \to \infty$, the region size n of the possible diagonal crack tip also tends to infinity. As a result, the first quotient under the square root vanishes. Therefore, for extremely large beams, $\mathrm{CoV}(\sigma_N)$ tends to the constant $\sqrt{\beta/\alpha}$, which is the coefficient of variation for $\sqrt{D_0}$.

Two remarks about this result should be made. First, we do not assume any specific type of distribution for D_0 or $\sqrt{D_0}$ in the foregoing derivation. The result is valid as long as $\sqrt{D_0}$ has a finite mean and variance. Second, this result relies on the assumption that σ_0 and D_0 are statistically independent. In reality, D_0 should have some degree of correlation with σ_0. Therefore, the large size limit of the strength CoV might not be exactly $\sqrt{\beta/\alpha}$. Because D_0 does not scale with D, D_0 and σ_0 cannot be fully coupled ($D_0 \propto \sigma_0$). According to this argument, the constant mean and standard deviation of D_0 will show up in the expression of $\mathrm{CoV}(\sigma_N)$ in a similar way as in the case of independence, which will lead to a nonzero strength CoV for $D \to \infty$.

With this large size constant CoV, we propose an approximate size effect equation for the nominal strength CoV, ω, for RC beams

$$\omega = \omega_0 \left[1 + \left(\frac{D_b}{D} \right)^r \right]^{\frac{1}{2r}} \qquad (17)$$

where D_b = characteristic length; and r = positive empirical constant. This formula can be seen as the asymptotic matching of two limiting cases: (1) ductile limit for small sizes ($D \to 0$), characterized by the ductile fiber bundle model with its strength CoV scaling as $D^{-1/2}$, and (2) constant CoV for large sizes ($D \to \infty$) with $\omega_0 = \sqrt{\beta/\alpha} = \mathrm{CoV}(\sqrt{D_0})$. The three typical beam sizes that we used in the simulations fall in the intermediate range of the size effect relation. Combining this with the Freudenthal reliability integral (Freudenthal 1956; Freudenthal et al. 1964), the current size effect relation [Eq. (17)] for strength CoV could further be used in the structural reliability analysis presented in Le and Bažant (2020) for the safety factor in RC beam design.

Conclusions

1. The simulations confirm that the ultimate failure of the RC beam is triggered by the compression-shear failure of a small region at the top of the beam. This is similar to the failure of the compression strut in the strut-and-tie model, which was observed to occur near the top of the beam and close to the tip of the diagonal crack (Yu et al. 2016; Dönmez and Bažant 2019; Bažant and Planas 1998).

2. Despite the fact that concrete is quasi-brittle, the reinforcement enables a stable propagation of the diagonal shear crack before the peak load is reached. Therefore, the weakest-link model for plain concrete does not apply.

3. The mean nominal strength of the RC beams follows the Type-2 size effect, which is deterministic and energetic.

4. Based on Monte Carlo simulations, the zone of the possible critical shear cracks becomes larger as the structure size increases, and its growth rate is smaller than D^2. Equivalently, as we rescale the structures strictly to the same size, the critical zone for the largest structure reduces to a point.

5. The basic idea advanced here is that the shear strength follows the distribution of the sample p-quantile of strengths in a small critical region, leading to a normal distribution for the large size limit.

6. The justification for this idea is that the number of critical material elements of random strength that can trigger failure grows with the size of the near-tip critical region. This region, in turn, is not constant but grows with structure size. Therefore, what matters is not the number but the percentage, or quantile, of the elements of random strength in the structure.

7. There is a significant size effect on the CoV of strength. The CoV of strength decreases as the structure size increases. However, the CoV decrease weakens at large sizes, and the large size limit of the CoV of strength is a constant.

Data Availability Statement

All data and finite element models that support the findings of this study are available from the corresponding author on reasonable request.

Acknowledgments

References

ACI (American Concrete Institute). 2019. *Building code requirements for structural concrete and commentary*. ACI 318-19. Farmington Hills, MI: ACI.

Bažant, Z., M. Hubler, M. Salviato, and J. Le. 2013. "Scaling of failure probability of quasibrittle structures with large cracks." In *Proc., 11th Int. Conf. on Structural Safety and Reliability, ICOSSAR 2013*, 955–958. Boca Raton, FL: CRC Press.

Bažant, Z. P. 1984. "Size effect in blunt fracture: Concrete, rock, metal." *J. Eng. Mech.* 110 (4): 518–535. https://doi.org/10.1061/(ASCE)0733-9399(1984)110:4(518).

Bažant, Z. P. 1997. "Fracturing truss model: Size effect in shear failure of reinforced concrete." *J. Eng. Mech.* 123 (12): 1276–1288. https://doi.org/10.1061/(ASCE)0733-9399(1997)123:12(1276).

Bažant, Z. P. 2002. *Scaling of structural strength*. London: CRC Press.

Bažant, Z. P., and M. Kazemi. 1990. "Determination of fracture energy, process zone length and brittleness number from size effect, with application to rock and concrete." *Int. J. Fract.* 44 (2): 111–131.

Bažant, Z. P., and B. H. Oh. 1983. "Crack band theory for fracture of concrete." *Matériaux et construction* 16 (3): 155–177. https://doi.org/10.1007/BF02486267.

Bažant, Z. P., and S.-D. Pang. 2006. "Mechanics-based statistics of failure risk of quasibrittle structures and size effect on safety factors." *Proc. Natl. Acad. Sci.* 103 (25): 9434–9439.

Bažant, Z. P., and S.-D. Pang. 2007. "Activation energy based extreme value statistics and size effect in brittle and quasibrittle fracture." *J. Mech. Phys. Solids* 55 (1): 91–131. https://doi.org/10.1016/j.jmps.2006.05.007.

Bažant, Z. P., and J. Planas. 1998. Vol. 16 of *Fracture and size effect in concrete and other quasibrittle materials*. London: CRC Press.

Bažant, Z. P., and Q. Yu. 2009. "Universal size effect law and effect of crack depth on quasi-brittle structure strength." *J. Eng. Mech.* 135 (2): 78–84. https://doi.org/10.1061/(ASCE)0733-9399(2009)135:2(78).

Bertin, E., and G. Györgyi. 2010. "Renormalization flow in extreme value statistics." *J. Stat. Mech: Theory Exp.* 2010 (8): P08022. https://doi.org/10.1088/1742-5468/2010/08/P08022.

Bolander, J., Jr., and S. Saito. 1998. "Fracture analyses using spring networks with random geometry." *Eng. Fract. Mech.* 61 (5–6): 569–591. https://doi.org/10.1016/S0013-7944(98)00069-1.

Caner, F. C., and Z. P. Bažant. 2013a. "Microplane model M7 for plain concrete. I: Formulation." *J. Eng. Mech.* 139 (12): 1714–1723. https://doi.org/10.1061/(ASCE)EM.1943-7889.0000570.

Caner, F. C., and Z. P. Bažant. 2013b. "Microplane model M7 for plain concrete. II: Calibration and verification." *J. Eng. Mech.* 139 (12): 1724–1735. https://doi.org/10.1061/(ASCE)EM.1943-7889.0000571.

Chao, S.-H. 2020. "Size effect on ultimate shear strength of steel fiber-reinforced concrete slender beams." *ACI Struct. J.* 117 (1): 145–158. https://doi.org/10.14359/51718018.

Cusatis, G., A. Mencarelli, D. Pelessone, and J. Baylot. 2011. "Lattice discrete particle model (LDPM) for failure behavior of concrete. II: Calibration and validation." *Cem. Concr. Compos.* 33 (9): 891–905. https://doi.org/10.1016/j.cemconcomp.2011.02.010.

Daluga, D., K. McCain, M. Murray, and S. Pujol. 2017. "Effect of geometric scaling on shear strength of reinforced concrete beams with stirrups." *ACI Struct. J.* 114 (6): 1397–1406.

Dönmez, A., and Z. P. Bažant. 2019. "Critique of critical shear crack theory for fib model code articles on shear strength and size effect of reinforced concrete beams." *Struct. Concr.* 20 (4): 1451–1463. https://doi.org/10.1002/suco.201800315.

Eliáš, J., M. Vořechovskỳ, J. Skoček, and Z. P. Bažant. 2015. "Stochastic discrete meso-scale simulations of concrete fracture: Comparison to experimental data." *Eng. Fract. Mech.* 135 (Feb): 1–16. https://doi.org/10.1016/j.engfracmech.2015.01.004.

Fisher, R. A., and L. H. C. Tippett. 1928. "Limiting forms of the frequency distribution of the largest or smallest member of a sample." In Vol. 24 of *Proc., Mathematical: Cambridge Philosophical Society*, 180–190. Cambridge, UK: Cambridge University Press.

Freudenthal, A. M. 1956. *Safety and the probability of structural failure*. Reston, VA: ASCE.

Freudenthal, A. M., J. M. Garrelts, and M. Shinozuka. 1964. *The analysis of structural safety*. New York: Columbia Univ.

Ghannoum, W. M. 1998. *Size effect on shear strength of reinforced concrete beams*. Ottawa: National Library of Canada.

Kendall, M. G., A. Stuart, and J. K. Ord. 1948. Vol. 1 of *The advanced theory of statistics*. 4th ed. Hoboken, NJ: Wiley.

Kim, J.-K., and Y.-D. Park. 1994. "Shear strength of reinforced high strength concrete beams without web reinforcement." *Mag. Concr. Res.* 46 (166): 7–16. https://doi.org/10.1680/macr.1994.46.166.7.

Kuo, W. W., T. T. Hsu, and S. J. Hwang. 2014. "Shear strength of reinforced concrete beams." *ACI Struct. J.* 111 (4): 809. https://doi.org/10.14359/51686733.

Kwak, Y.-K., M. O. Eberhard, W.-S. Kim, and J. Kim. 2002. "Shear strength of steel fiber-reinforced concrete beams without stirrups." *ACI Struct. J.* 99 (4): 530–538.

Le, J.-L., and Z. P. Bažant. 2020. "Failure probability of concrete specimens of uncertain mean strength in large database." *J. Eng. Mech.* 146 (6): 04020039. https://doi.org/10.1061/(ASCE)EM.1943-7889.0001770.

Le, J.-L., Z. P. Bažant, and M. Z. Bazant. 2011. "Unified nano-mechanics based probabilistic theory of quasibrittle and brittle structures. I. Strength, static crack growth, lifetime and scaling." *J. Mech. Phys. Solids* 59 (7): 1291–1321. https://doi.org/10.1016/j.jmps.2011.03.002.

Leadbetter, M. R., G. Lindgren, and H. Rootzén. 2012. *Extremes and related properties of random sequences and processes*. New York: Springer.

Luo, W., and Z. P. Bažant. 2018. "Fishnet model with order statistics for tail probability of failure of nacreous biomimetic materials with softening interlaminar links." *J. Mech. Phys. Solids* 121 (Dec): 281–295. https://doi.org/10.1016/j.jmps.2018.07.023.

Luo, W., and Z. P. Bažant. 2019. "Fishnet statistical size effect on strength of materials with nacreous microstructure." *J. Appl. Mech.* 86 (8): 1–10. https://doi.org/10.1115/1.4043663.

Mahmoud, K., and E. El-Salakawy. 2016. "Size effect on shear strength of glass fiber-reinforced polymer-reinforced concrete continuous beams." *ACI Struct. J.* 113 (1): 125–134. https://doi.org/10.14359/51688065.

Man, H.-K., and J. Van Mier. 2011. "Damage distribution and size effect in numerical concrete from lattice analyses." *Cem. Concr. Compos.* 33 (9): 867–880. https://doi.org/10.1016/j.cemconcomp.2011.01.008.

Mood, A. M. 1950. *Introduction to the theory of statistics*. New York: Wiley.

Samuel-Cahn, E. 1994. "Combining unbiased estimators." *Am. Stat.* 48 (1): 34–36.

Sherwood, E. G. 2008. *One-way shear behaviour of large, lightly-reinforced concrete beams and slabs*. Ann Arbor, MI: ProQuest.

Stigler, S. M. 1973. "Studies in the history of probability and statistics. XXXII: Laplace, Fisher, and the discovery of the concept of sufficiency." *Biometrika* 60 (3): 439–445.

Syroka-Korol, E., J. Tejchman, and Z. Mróz. 2014. "FE analysis of size effects in reinforced concrete beams without shear reinforcement based on stochastic elasto-plasticity with non-local softening." *Finite Elem. Anal. Des.* 88 (Oct): 25–41. https://doi.org/10.1016/j.finel.2014.05.005.

Walker, H. M. 1943. *Elementary statistical methods*. New York: Springer.

Weibull, W. 1939. "A statistical theory of strength of materials." *R. Swedish Inst. Eng. Res.* 151 (15): 1–45.

Yu, Q., J.-L. Le, M. H. Hubler, R. Wendner, G. Cusatis, and Z. P. Bažant. 2016. "Comparison of main models for size effect on shear strength of reinforced and prestressed concrete beams." *Struct. Concr.* 17 (5): 778–789. https://doi.org/10.1002/suco.201500126.